Type I Mid-Infrared MQW Lasers using AlInAsSb barriers and InAsSb wells

Leslie G. Vaughn*[a], L. Ralph Dawson[a], Edwin A. Pease[b], Luke F. Lester[a], Huifang Xu[c], Yingbing Jiang[c], Alan L. Gray[b]
[a]Center for High Technology Materials, UNM, 1313 Goddard SE, Albuquerque, NM 87106;
[b]Zia Laser, Inc., 801 University Blvd. SE, Suite 105, Albuquerque, NM 87106;
[c]Dept. of Earth and Planetary Science, MSCO3-2040, 1 University of New Mexico, Albuquerque, NM 87131-0001

ABSTRACT

For many years, mid-infrared (2-5μm) semiconductor lasers operating at or near room temperature have been sought for use in LADAR, gas sensing, and spectroscopy. Smaller bandgap materials necessary for this range are more susceptible to non-radiative Auger recombination. Further, as laser structures become more complicated, like quantum cascade intersubband and interband lasers, Shockley-Read-Hall losses increase. The simplest structure is Type-I multiple quantum well (MQW), but few QW III-V heterojunction material systems capable of 2-5μm emission have a Type-I offset. One such system with InAsSb wells and AlInAsSb barriers has been unable to exceed 175K under CW operation partially due to poor carrier confinement associated with small valence band offsets. This paper describes the growth and performance of AlInAsSb/InAsSb lasers using a 0.3 mole fraction of Al in the Group III elements. Increased Al content enhances the valence and conduction band offsets, but the AlInAsSb alloy exhibits a miscibility gap above 0.06 Al mole fraction, so a digital alloy technique was used to grow high quality 0.3-2μm thick quaternary films. As Al mole fraction in the barriers was increased from 0.20 to 0.30 an 80-fold increase in photoluminescence (PL) was observed. The corresponding lasers were grown and tested demonstrating lasing at 3.9μm and 50K. Theoretical studies suggest that adding Ga to the barriers, forming an AlGaInAsSb quinary alloy, results in band structures more favorable towards minimizing Auger effects and realizing Type I offset behavior over a wider range of alloy compositions. PL structures were grown and tested, again using a digital alloy technique for the quinary alloy. Preliminary results show promise.

Keywords: Mid-infrared, Type-I laser, AlInAsSb, InAsSb, AlGaInAsSb, digital alloy, quaternary, quinary

1. INTRODUCTION

The search for material systems that will produce high power, room temperature mid-infrared (IR) semiconductor diode lasers operating between 2 and 5 microns has been of particular interest over the last 15 years. These lasers find uses in field communications, laser radar, pollution monitoring, remote toxic gas sensing and molecular spectroscopy. Some inherent challenges to achieving this goal remain. Longer wavelength materials have smaller bandgaps making them more susceptible to Auger recombination. Consequently, they must be operated well below room temperature to decrease the probability of this multi-step process. Also, most of the material systems capable of this wavelength range have a Type II, broken or staggered band offset, leading to poorer carrier confinement, lower efficiencies and higher thresholds than Type I nested band offset systems. AlInAsSb/InAsSb is one of the few material systems with a predicted Type I band offset.

To decrease Auger recombination and increase operating temperature, three strategies can be used. One is to add compressive strain to the well. Strain separates energy levels in the valence band which increases confinement. This separation causes a decrease in the hole density of states, and results in a decrease in the number of intermediate and final energy states available for Auger. Another strategy to higher operating temperature, Type I mid-IR InAsSb/AlInAsSb lasers is to increase the aluminum content in the barriers. This approach increases both the conduction and valence band offsets by increasing the quaternary barrier bandgap. The third strategy that has been suggested to decrease Auger recombination is the addition of a fifth element, gallium, to the barrier alloy to make a

Physics and Simulation of Optoelectronic Devices XIII, edited by Marek Osinski, Fritz Henneberger, Hiroshi Amano, Proc. of SPIE Vol. 5722 (SPIE, Bellingham, WA, 2005)
0277-786X/05/$15 · doi: 10.1117/12.606226

quinary[1]. The presence of the fifth element may help by altering the subband structure of the valence band, decreasing the hole density of states.

Although the quaternary AlInAsSb barrier/InAsSb well conduction and valence band offsets are predicted to be Type I, the valence band offset is small, so hole confinement is a concern. Higher aluminum content in the barrier increases the conduction and valence band offsets. The splitting of the heavy and light-hole energy subbands using compressive strain is another tool for increasing the valence band offset. However, the tradeoff of larger compressive strain for a given InAsSb composition is a larger energy gap and shorter emission wavelength[2]. Given a GaSb substrate, the net effect of these composition adjustments in the well and barrier, is that adding compressive strain by adding more Sb to the well alloy and increasing aluminum content in the barrier increase the valence band offset.

Below room temperature MQW lasers with $Al_{0.15}In_{0.85}As_{0.9}Sb_{0.1}$ barriers and InAsSb wells on InAs and $Al_{0.1}In_{0.9}As_{0.9}Sb_{0.1}$ barriers and InAsSb wells on GaSb have been demonstrated at 3.5 and 3.9 microns, respectively[3, 4]. An objective of the current work is to examine the impact and challenges of further increasing the aluminum content in the barrier. As well as increasing band offsets, increased aluminum content will decrease the index of refraction, degrading the optical confinement within the laser. In addition, a miscibility gap is predicted for the quaternary alloy at aluminum fractions of 0.06 and greater for material lattice-matched to GaSb substrates and 0.12 and greater for material lattice-matched to InAs substrates. Growth of material beyond these limits is predicted to phase separate under equilibrium or near-equilibrium growth conditions and has been observed for non-equilibrium MBE growth[5]. Despite these challenges, the thesis is that the increase in carrier confinement due to improved Type I behavior by adding more aluminum to the AlInAsSb barrier will improve the laser performance.

Prior research into the growth of AlInAsSb has yielded some instructive results. In related HEMT and kinetic heterojunction research, single phase thin film AlInAsSb alloys have been grown well into the miscibility gap at temperatures around 350°C using molecular beam epitaxy (MBE)[6, 7] and metal organic vapor phase epitaxy (MOVPE)[8] systems. However, that temperature is not suitable for the AlInAsSb/InAsSb laser structure because InAsSb must be grown above 400 - 430°C to avoid atomic ordering[9-12]. The phenomena of atoms naturally ordering into lamella of alternating composition is undesirable because the degree to which it occurs is unpredictable, usually occurring in patches throughout the alloy, and the resulting film has a reported smaller bandgap than expected for the random alloy. It should also be noted that the phase stability diagram for the quinary is bounded by quaternary phase stability diagrams with large miscibility gaps—at least for the alloys with both As and Sb—so it is expected that the quinary will have large regions of immiscibility also.

Since MBE has the capability of growing under near-equilibrium to far-from-equilibrium conditions, this flexibility can be exploited to promote single-phase growth of alloys within the miscibility gap. This paper describes the digital alloy approach used to grow stable $Al_xIn_{(1-x)}As_ySb_{(1-y)}$ micron-thick films lattice-matched to the GaSb substrates for quaternary alloy aluminum fractions, x = 0.05 to 0.5, well into the miscibility gap. Further, this digital alloy technique used for the quaternary can easily accommodate the addition of GaSb itself into the film sequence to make a quinary that it also lattice-matched to GaSb. Quinary films have been grown and tested with the optical results presented in this paper. Also described here are results from optical testing of active regions and complete laser structures within these material systems.

2. EXPERIMENT

All samples were grown using a VG V80H solid source MBE system. Digital alloy films were grown using a sequence of binaries, while random alloys of nominally the same composition were grown with all source shutters open, for comparison. AlSb, InSb and InAs films were used to grow the quaternary digital alloy. Since the sticking coefficients of the Group V elements are less than unity and As tends to leak around the shutter and displace some of the bonded Sb during growth, the mole fractions y and (1-y) are not only influenced by layer thicknesses but also by the ratio of the beam equivalent pressures (BEPs). The ratio of these pressures and the ratio of the InSb to InAs thicknesses were used to adjust the Group V composition until GaSb lattice-match conditions were achieved. The quinary was grown in the same fashion with the addition of a thin layer of GaSb in the digital alloy sequence. The overall thickness of the films was one micron and the digital alloy period was 1.5 - 2.5nm. Both Group V elements were supplied by valved cracker

sources run at sufficiently high temperatures to produce predominantly As_2 and Sb_1. The ratio of BEPs for As to Sb was maintained at 4:3, and the Group V to Group III BEP ratios were 5:1 for As to In, 13:1 for Sb to Al, and 4:1 for Sb to In. Both aluminum and indium growth rates were 0.75ML/sec and the gallium growth rate was maintained at 0.5ML/sec.

Quaternary random alloys and digital alloys were grown in the temperature range of 460-520°C, with most being grown at an optimal temperature of 480°C. All quinary alloys were grown at 480°C. The substrate temperature was monitored using an optical pyrometer. The temperature range was chosen to be low enough to ensure that all Group III elements would have a sticking coefficient of approximately one, and high enough to ensure that InAsSb would be single phase with no atomic ordering.

For most samples, composition was determined using calibrated Group III growth rates and double crystal X-ray diffraction (DCXRD). These growth rates were calibrated using refractive high-energy electron diffraction (RHEED) oscillations and binary film thickness fringes from DCXRD. Periodically, sample compositions were verified using Rutherford Backscattering Spectroscopy (RBS) or Secondary Ion Mass Spectroscopy (SIMS).

Photoluminescence (PL) was generated using a 980nm-laser diode pump array and measured with a scanning monochrometer and an InSb detector. The sample was mounted in a liquid nitrogen-cooled cryostat chamber. The same equipment was used to optically-pump the edge-emitting lasers and measure the output.

3. DISCUSSION

In order to achieve larger Type I band offsets with InAsSb wells and AlInAsSb barriers, it is necessary to increase the aluminum mole fraction in the barrier quaternary. With the existence of the miscibility gap, going beyond 0.06 mole fraction aluminum requires an alternative approach to bulk growth. A digital alloy technique is used. Digital alloys, sometimes referred to as ultrathin superlattices, employ the technique of growing alternating thin layers of stable binaries, ternaries and/or quaternaries. When the layers within the digital alloy period are thin enough, on the order of a few monolayers, the resulting film properties are approximately those of a bulk alloy with the average composition of the film[13].

3.1 AlInAsSb digital alloy growth and characterization

In this study, AlInAsSb digital alloys are grown using alternating layers of InAs, InSb and AlSb. The overall composition of the film is determined by the ratio of the thicknesses of these layers. Stable, single-phase binaries were chosen for the layers with the advantage of having only one Group V element in each, thus avoiding competing Group V elements in any particular layer, making the layers more uniform and reproducible. Further, lattice-match of the overall film to the GaSb substrate is simply controlled by adjusting the ratio of InAs and InSb layer thicknesses.

One-micron thick films were grown lattice-matched to the GaSb substrate with aluminum mole fractions of 0.2, 0.3 and 0.4. The digital alloy period was 1.5 to 2.0 nm thick with each binary layer between 0.5-5.0 monolayers. The composition, thickness, digital alloy period and crystal quality of the digital alloy quaternary films were evaluated using DCXRD and transmission electron microscopy (TEM).

3.1.1 Crystal Quality

Symmetrical (004) x-ray diffraction scans were performed for each DA quaternary alloy. Typical scans are shown in Figure 1. All DA films have 0^{th} order peaks with full-width half maximum (FWHM) values less than or equal to two times the FWHM value for the substrate peak. The more lattice imperfections there are, the larger the FWHM values. The closer the grown film values are to the substrate values, the better the crystal quality of the grown film. Figure 1(a) also shows the thickness fringes associated with the DA period thickness. Figure 1(b) shows the thickness fringes corresponding to the overall thickness of the DA film, in this case 1 micron. The presence of many distinguishable orders of thickness fringes signifies fewer defects in the film.

(a) (b)

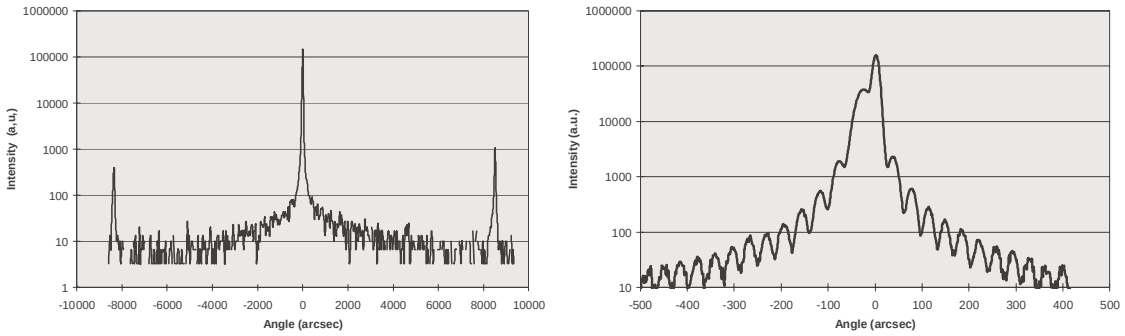

Figure 1. (a) (004) DCXRD scan of an $Al_{0.32}In_{0.68}As_{0.62}Sb_{0.38}$ DA sample showing the thickness fringes corresponding to the digital alloy period, (b) same showing the thickness fringes corresponding to the overall quaternary film thickness.

Further verification of the film crystal quality is given by the TEM micrograph in Figure 2. Here the layers within the digital alloy are visible and are seen to be very uniform. The lighter regions are In-rich, corresponding to the InAs and InSb layers and the darker regions are Al-rich, corresponding to the AlSb layer.

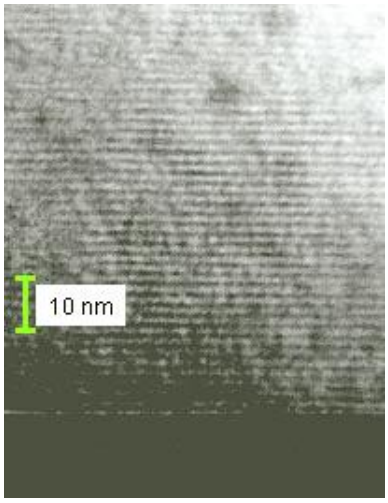

Figure 2. Map of Indium in a 30% aluminum quaternary DA sample using Energy-filtering transmission electron microscopy (TEM). The bright regions indicate indium-rich layers.

3.1.2 Thermal stability

Thermal stability is a concern because given enough time and temperature, the alloy will phase change to its equilibrium configuration and, in this case, that is multiphase. A sample was evaluated with DCXRD, then stored at room temperature for 1 year and re-evaluated. There was no discernable change in the DCXRD results. To accelerate the phase change due to temperature, 0.3 aluminum mole fraction AlInAsSb digital alloys were prepared and subjected to different temperatures for different amounts of time. The results are shown in Figure 3. The samples that saw 400ºC for different times do show a slight degradation in film quality as the 0^{th} order alloy peak shifts away from the substrate peak, but after 30 minutes at 400ºC, the sample peak is still within approximately 100 arcsec of the substrate peak. The second plot shows two samples heated for 10 minutes, one at 400ºC and one at 450ºC. The 450ºC sample is beginning to show a little degradation but the peak is still well within the 100 arcsec range of the substrate peak. So, as expected,

given time and temperature, there will be some changes to the alloy. The extent of the changes and the affect on the laser performance merits further study.

a)

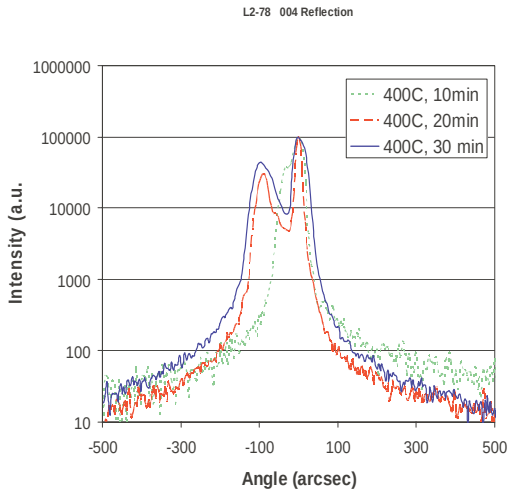

b)

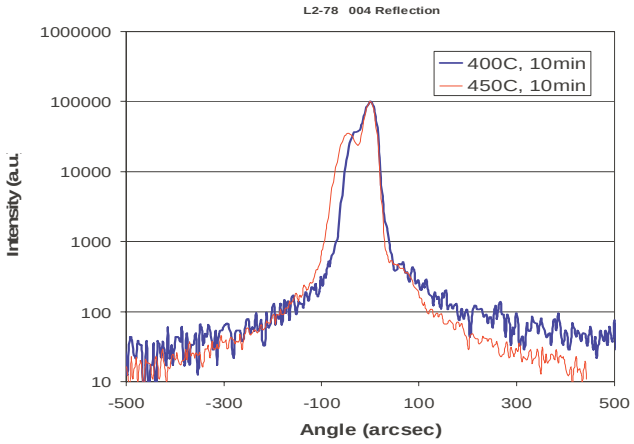

Figure 3. Thermal study of a $Al_{0.3}In_{0.7}AsSb$ digital alloy film at (a.) 10-30 minutes at 400°C, and (b) 10 minutes at 400°C and 450°C.

3.2 Type I Active Region: InAsSb wells and AlInAsSb barriers

All samples are grown with InAsSb wells and AlInAsSb digital alloy barriers on a GaSb substrate. The waveguide is the same composition as the barriers, and the clad is $Al_{0.9}Ga_{0.1}As_{0.08}Sb_{0.92}$. The structure growth temperature was 480°C. The barriers, waveguide and clad are lattice-matched to the GaSb substrate. This allows all of the compressive strain to be confined to the wells. The wells are 10nm wide, with 30nm barriers on either side of each well. The rest of the layers are the thicknesses listed in Figure 4. All reported PL and laser samples have 4-10 quantum wells in the active region. PL samples are grown only through the top AlInAsSb waveguide, while lasers include the top clad and GaSb cap.

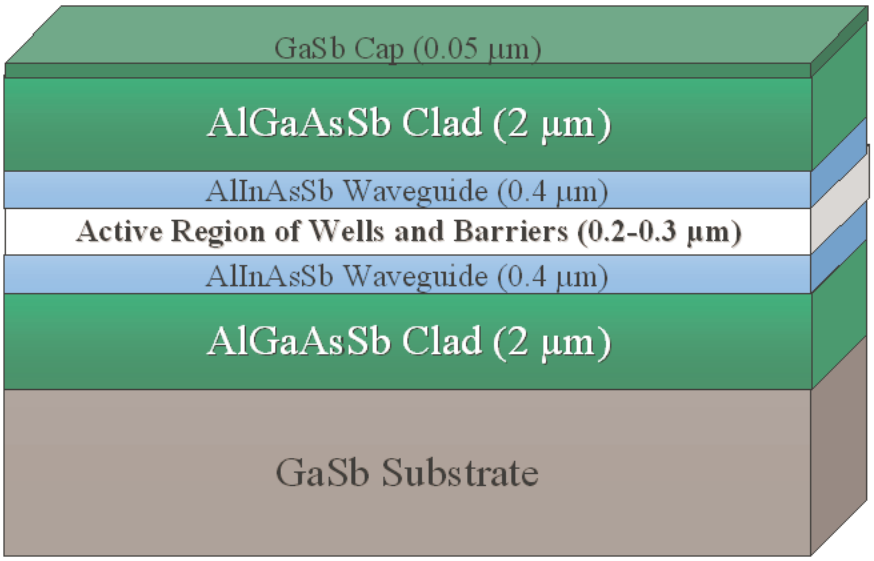

Figure 4. Type I mid-IR laser structure

3.2.1 Effects of increasing aluminum concentration in AlInAsSb barriers

Stable digital alloy quaternary films make it possible to add aluminum to the barriers to achieve compositions throughout the miscibility gap. Several samples of different quaternary aluminum mole fraction have been successfully grown in PL structures and tested. For these samples, the photoluminescence was measured at 92K. The wells have 0.97% compressive strain at a composition of $InAs_{0.77}Sb_{0.23}$ and the aluminum mole fraction in the quaternary digital alloy is 0.2, 0.3 and 0.4. The results of the PL measurements are shown in Figure 5. There is a blue shift in wavelength with increasing aluminum because as the aluminum fraction increases, the barrier bandgap becomes larger, increasing the confinement energies.

The values for the 0.2 aluminum mole fraction barriers have been multiplied by 20 so that the peak is recognizable in the range of this graph. The PL intensity increase between 0.3 and 0.2 aluminum mole fraction is almost two orders of magnitude and corresponds to increased hole confinement with increasing aluminum content. This is consistent with theoretical predictions. The magnitude of this increase suggests a transition from Type II behavior to Type I behavior.

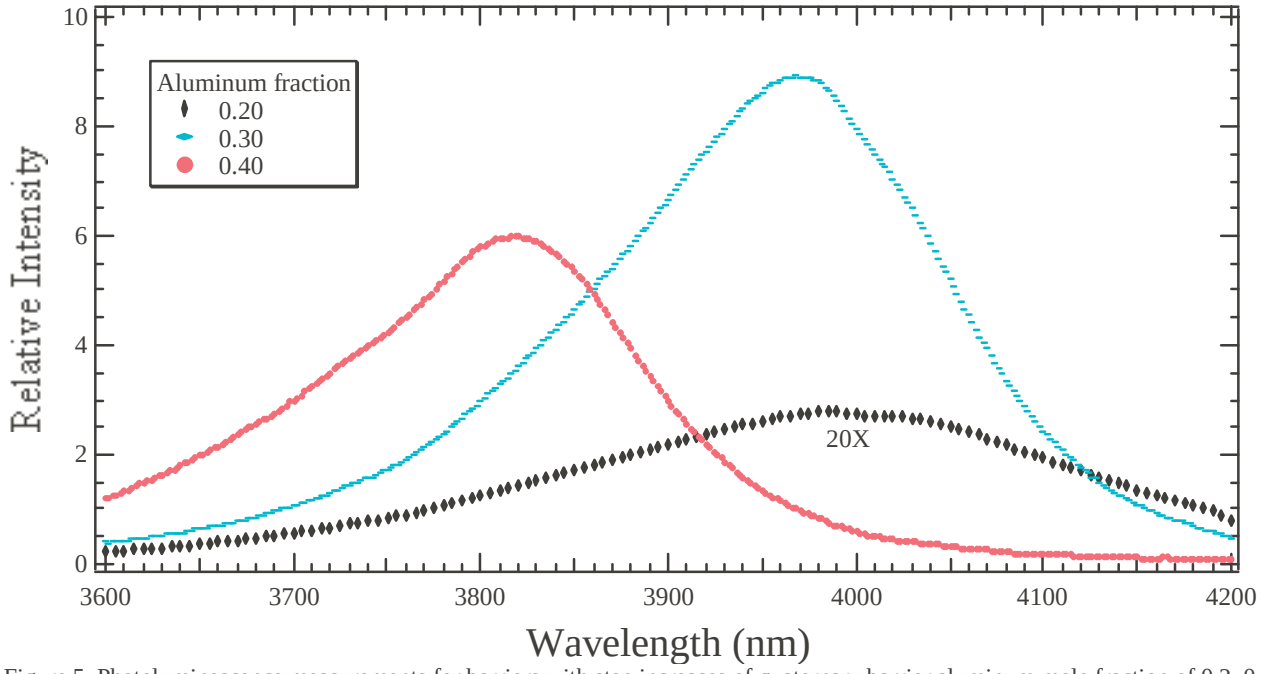

Figure 5. Photoluminescence measurements for barriers with step increases of quaternary barrier aluminum mole fraction of 0.2, 0.3 and 0.4.

3.2.2 Effects of increasing well strain

The addition of well strain should also decrease Auger losses and increase the valence band offset to achieve more radiative active regions that operate at higher temperatures. The strain in the wells is increased by adding more Sb to the well alloy. This not only increases strain in the wells, but increases wavelength. Auger losses are probably decreased because the compressive strain splits the heavy and light hole subbands. The experimental results of adding strain are shown in Figure 6. The brightest PL comes from the wells with ~1% compressive strain while the weakest PL is from the sample with the lowest amount of compressive strain (0.3%). Again, there is an increase in PL intensity of almost two orders of magnitude. This is also consistent with a change from Type II behavior to Type I behavior.

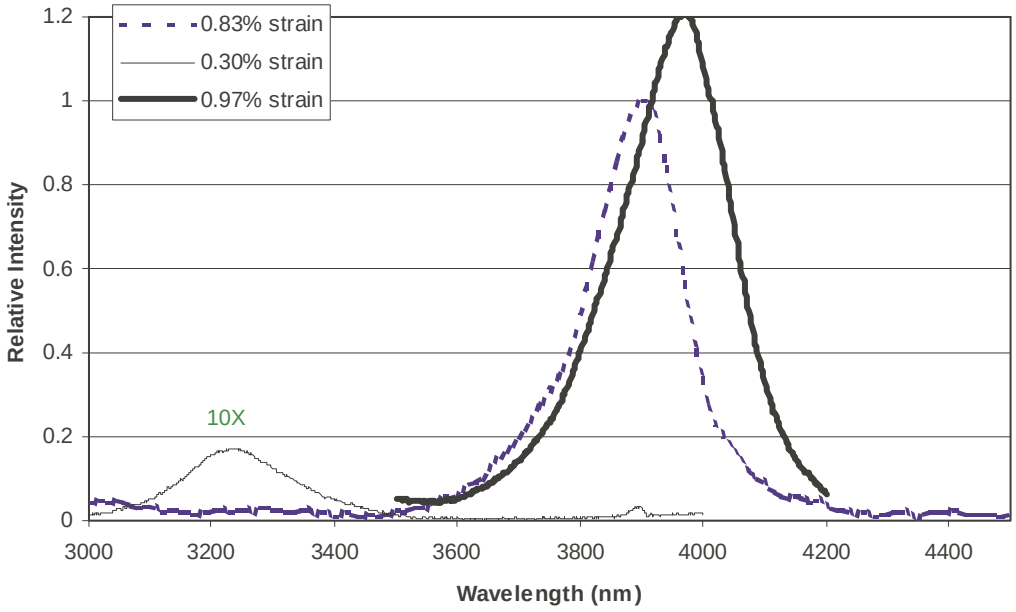

Figure 6. Photoluminescence measurements for step increases in compressive strain in the well with $Al_{0.3}In_{0.7}AsSb$ barriers

3.3 Type I mid-IR lasers

The lasers are all grown as indicated in Figure 4 with the active region as described in section 3.2. The highest PL intensity combination of quaternary barrier composition and compressive well strain corresponds to an active region with 0.8-1.0% compressive strain in the wells and 0.3 aluminum mole fraction in the quaternary barriers. Lasers were grown and tested with these design criteria. Each laser was thinned and mounted on a copper H-mount using indium solder. The mount was then placed on a cold finger in a cryostat chamber, the chamber was evacuated and the laser was cooled to 50K. The 2.5mm cavity Type I mid-IR GaSb-based laser was optically pumped using a 980nm laser diode array with a 0.5% duty cycle and a 50μs pulse width. The results are shown in Figure 7. The inset shows the 3.9μm emission spectrum as the laser was pumped with increasing power. The maximum operating temperature for this laser was 80K. For comparison, lasers were grown with 0.3% well strain and 0.3 aluminum mole fraction in the quaternary barriers. However, these lasers only exhibited superluminescence and did not lase. It is expected that increasing strain further will improve the operating characteristics, but there is a limit to how much strain the structure can contain before deleterious defect levels are reached. PL results suggest laser performance should be improved over reported results for this material system and it is possible that the thermal stability of the digital alloy barriers is affecting the active region. So, additional improvement may come after the active region is grown by lowering the growth temperature for the remaining clad.

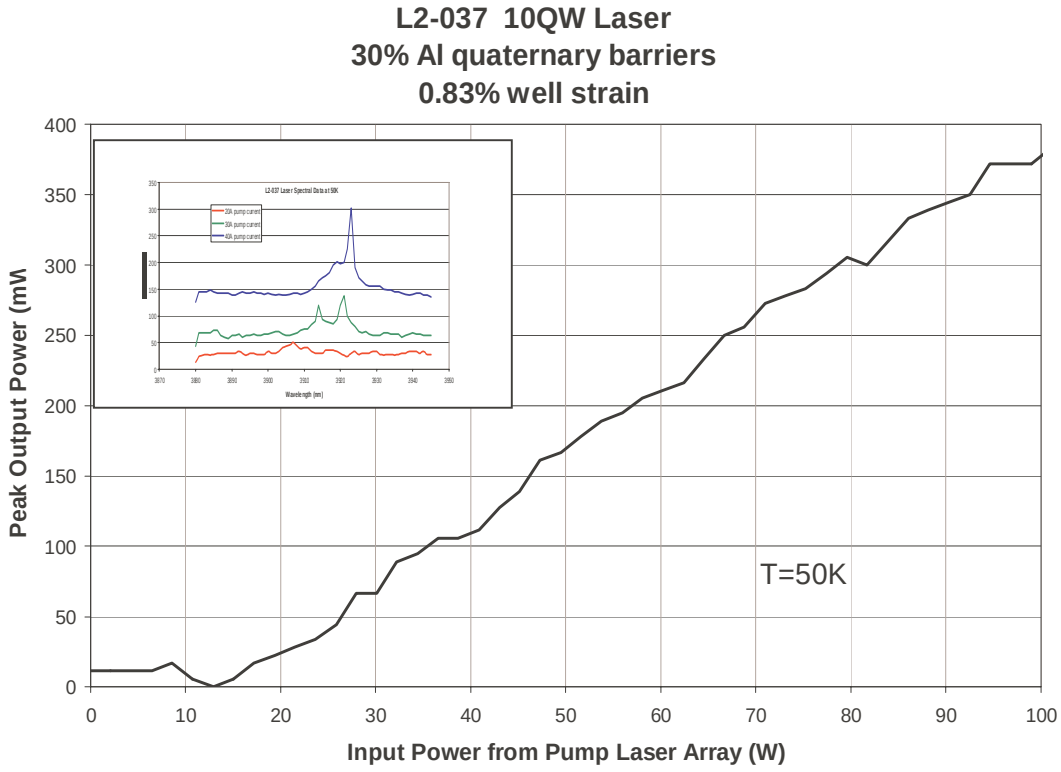

Figure 7. L-I curve for 0.83% compressively strained InAsSb wells with $Al_{0.3}In_{0.7}AsSb$ barriers.

3.4 Quinary barrier

Theoretical studies suggest that adding a fifth element to the barrier alloy will result in a subband structure that will decrease the Auger recombination. Since this is the most common mechanism for non-radiative recombination in small bandgap materials, a reduction in Auger should increase the operating temperature of the device. The digital alloy technique makes this a very straightforward next step. Quaternary digital alloys have already been lattice-matched to GaSb. By adding a thin layer of GaSb in the digital alloy sequence, the fifth element can easily be added to the alloy without disturbing the lattice-match condition.

One-micron thick films of $Al_{0.4}Ga_{0.15}In_{0.45}AsSb$ digital alloy, near lattice-matched to GaSb, were grown and evaluated. Although the growth was not optimized, XRD and TEM results are similar to those for the quaternary digital alloy. The FWHM of the 0^{th} order alloy peak was about 2X that of the substrate FWHM. TEM micrographs showed very regular layers, as with the quaternary.

Photoluminescence results of the quinary are shown in Figure 8(a). Of particular interest is that the quaternary alloy is predicted to become indirect somewhere between 0.3 and 0.5 mole fraction aluminum. By adding Ga to the alloy and observing photoluminescence, it appears that the alloy with this composition is direct bandgap.

This quinary digital alloy was then used as a barrier material with InAsSb wells in a laser structure complete with top clad. The sample was tested for photoluminescence and the results are shown in Figure 8(b). The quinary peaks were identified in each plot, and the InAsSb QW active region was observed in the 3.5-4.5μm emission range. Although this output was very weak, of particular interest is that the room temperature intensity is double that observed at 90K. In general, the cooler a Type I MQW mid-IR laser is during operation, the stronger the emission, again because of Auger.

This sample was then thinned and tested as a laser. However, no lasing or superluminescence was observed possibly due to the reduction of the valence band offset from the introduction of Ga into the barrier alloy.

a)

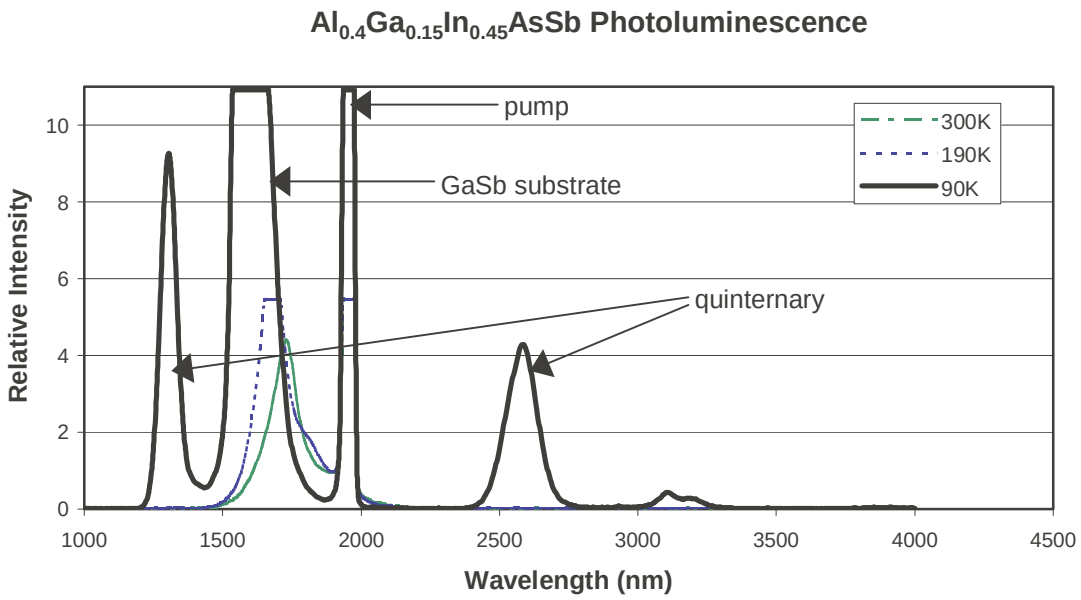

b)

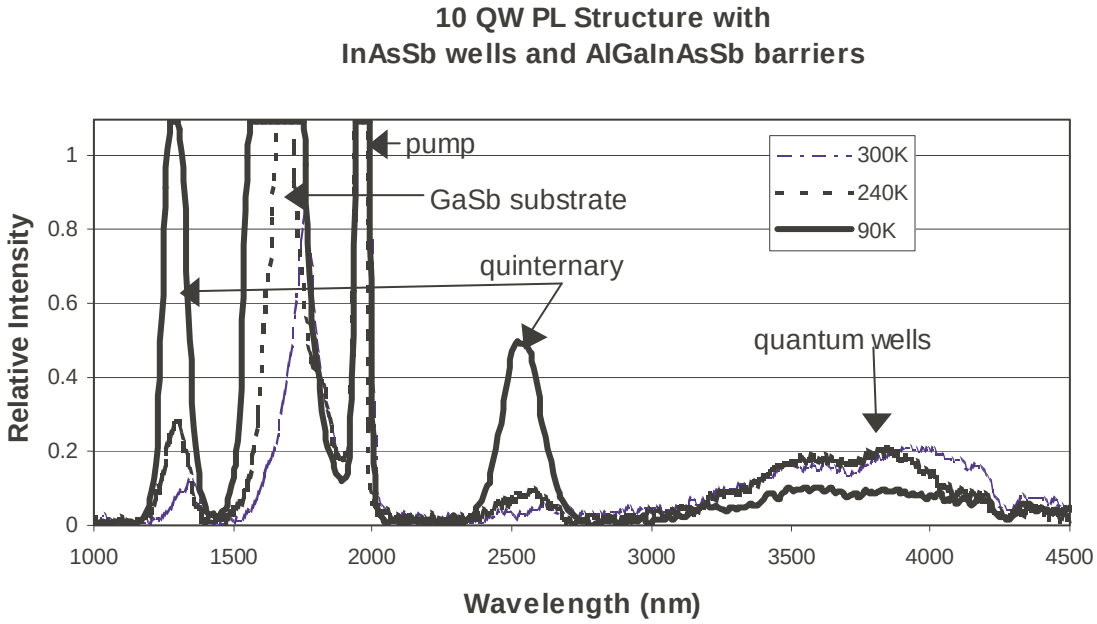

Figure 8. PL from (a) $Al_{0.4}Ga_{0.15}In_{0.45}As_{0.42}Sb_{0.58}$ 1-micron film and (b) from a MQW laser structure with $Al_{0.4}Ga_{0.15}In_{0.45}As_{0.42}Sb_{0.58}$ barriers and 0.9% compressively strained InAsSb wells.

4. CONCLUSIONS

AlInAsSb quaternary alloys were successfully grown using a digital alloy technique to achieve relatively stable high-aluminum compositions well within the miscibility gap. Evaluation of the resulting films verified the crystal quality. These films were then incorporated as barriers into the active region of a Type I laser structure with InAsSb wells. When quaternary alloys with increased aluminum mole fraction, from 0.2 to 0.3, were used, the 80X PL intensity increase suggests a transition from Type II to Type I behavior, as predicted. Adding strain to the well by increasing the Sb concentration also resulted in a substantial increase in PL intensity, also suggesting a transition from Type II to Type I behavior.

Active regions with 0.8% compressive well strain and 30% aluminum quaternary DA barriers were then grown in a laser structure with an AlInAsSb waveguide and AlGaAsSb clads. This structure was optically pumped under pulsed conditions and demonstrated lasing at 50K with an emission wavelength of 3.9μm. A maximum operating temperature of 80K was observed. More well strain may improve the operating characteristics, and reduction of growth temperature during top clad growth may alleviate some suspected degradation of the barriers in the active region. Further study is warranted.

In an effort to increase the effect on valence band offset, and reduce the effects of Auger recombination Ga was added to the barrier digital alloy. While not resulting in a functional laser, preliminary tests using an AlGaInAsSb quinary DA barrier material with the InAsSb wells showed a weak 3.5-4μm photoluminescence to be twice as intense at room temperature compared to 90K.

ACKNOWLEDGEMENTS

This material is based on research sponsored by the Air Force Research Laboratory, under the agreement number F49620-99-1-0330, and on research sponsored by the Office of Naval Research, under Grant # N00014-99-1-1023. The U. S. Government is authorized to reproduce and distribute reprints for Governmental purposes notwithstanding any copyright notation thereon. The views and conclusions contained herein are those of the authors and should not be interpreted as necessarily representing the official policies, endorsements or views, either expressed or implied, of the Air Force Research Laboratory, the Office of Naval Research or the U. S. Government.

REFERENCES

1. M. E. Flatte, J. T. Olesberg, S. A. Anson, T. F. Boggess, T. C. Hasenberg, R. H. Miles and C. H. Grein, "Theoretical performance of mid-infrared broken-gap multilayer superlattice lasers", *Appl. Phys. Lett.* **70**, 3212-3214, 1997.
2. L. A. Coldren and S. W. Corzine, in *Diode Lasers and Photonic Integrated Circuits*, p. 532, John Wiley & Sons, Inc., New York, 1995.
3. H. K. Choi and G. W. Turner, "InAsSb/InAlAsSb strained quantum-well diode lasers emitting at 3.9μm", *Appl. Phys. Lett.* **67**, 332-334, 1995.
4. H. K. Choi, G. W. Turner, M. J. Manfra and M. K. Connors, "175K continuous wave operation of InAsSb/InAlAsSb quantum-well diode lasers emitting at 3.5μm", *Appl. Phys. Lett.* **68**, 2936-2938, 1996.
5. G. W. Turner, M. J. Manfra, H. K. Choi and M. K. Connors, "MBE growth of high-power InAsSb/InAlAsSb quantum-well diode lasers emitting at 3.5μm", *J. Crystal Growth* **175/176**, 825-832, 1997.
6. M. Kudo and T. Mishima, "MBE growth of Si-doped InAlAsSb layers lattice-matched to InAs", *J. Crystal Growth* **175**, 844-848, 1997.
7. D. Washington, T. Hogan, P. Chow, T. Golding, C. Littler and U. Kirschbaum, "$Al_x In_{1-x} As_{1-y} Sb_y$/GaSb heterojunctions and multilayers grown by molecular beam epitaxy for effective-mass superlattices", *J. Vac. Sci. Technol. B* **16**, 1385-1388, 1998.
8. J. R. Chang, Y. K. Su, D. H. Jaw, H. P. Shiao, W. Lin, "Metalorganic vapor phase epitaxy (MOVPE) growth and characterization of AlInAsSb and AlInAsSb/InGaAs multiple-quantum-well structures", *J. Crystal Growth* **203**, 481-485, 1999.

9. T. Y. Seong, A. G. Norman, I. T. Ferguson and G. R. Booker, "Transmission electron microscopy and transmission electron diffraction structural studies of heteroepitaxial $InAs_y Sb_{1-y}$ molecular-beam epitaxial layers", *J. Appl. Phys.* **73**, 8227-8236, 1993.
10. S. R. Kurtz and R. M. Biefeld, "Magnetophotoluminescence of biaxially compressed InAsSb quantum wells", *Appl. Phys. Lett.* **66**, 364-366, 1995.
11. S. R. Kurtz, R. M. Biefeld and L. R. Dawson, "Modification of valence-band symmetry and Auger threshold energy in biaxially compressed $InAs_{1-x}Sb_x$ ", *Phys. Rev. B* **51**, 7310-7313, 1995.
12. S. R. Kurtz, R. M. Biefeld and A. J. Howard, "Magneto-optical determination of light-heavy hole splittings in As-rich InAsSb alloys and superlattices", *Appl. Phys. Lett* **67**, 3331-3333, 1995.
13. R. Kaspi and G. P. Donati, "Digital alloy growth in mixed As/Sb heterostructures", *J. of Crystal Growth* **251**, 515-520, 2003.